Self-Consistent Subband Calculations of AlGaN/GaN Single Heterojunctions

Kyu-Seok Lee, Doo-Hyeb Yoon, Sung-Bum Bae, Mi-Ran Park, and Gil-Ho Kim

We present a self-consistent numerical method for calculating the conduction-band profile and subband structure of AlGaN/GaN single heterojunctions. The subband calculations take into account the piezoelectric and spontaneous polarization effect and the Hartree and exchange-correlation interaction. We calculate the dependence of electron sheet concentration and subband energies on various structural parameters, such as the width and Al mole fraction of AlGaN, the density of donor impurities in AlGaN, and the density of acceptor impurities in GaN, as well as the electron temperature. The electron sheet concentration was sensitively dependent on the Al mole fraction and width of the AlGaN layer and the doping density of donor impurities in the AlGaN. The calculated results of electron sheet concentration as a function of the Al mole fraction are in excellent agreement with some experimental data available in the literature.

I. INTRODUCTION

Recent advances in the growth technology of III-nitride semiconductors have led to the development of AlGaN/GaN electrical devices for applications of high power and high frequency amplifiers for mobile and satellite communications and for other applications, such as actuators and sensors operated in harsh environments. Since GaN has a large bandgap of 3.4 eV [1], a high electron saturation velocity of about 3×10^7 cm/s [2], a high breakdown field of about 2×10^6 V/cm [3], and a small dielectric coefficient of 10 [4], AlGaN/GaN heterostructure field-effect transistors (HFETs) have shown a better performance in high power and high temperature operations than other conventional devices based on Si, GaAs, and InP. AlGaN/GaN HFETs fabricated on SiC substrates revealed output-power density of 9.1 W/mm at 8.2 GHz [5], while AlGaN/GaN HFETs fabricated on sapphire substrates showed output-power density of 8 W/mm at 9.5 GHz [6].

A typical HFET based on the Ga-faced AlGaN/GaN single heterojunction, even without intentional doping, has an ability to achieve a high electron sheet concentration of about 1×10^{13} electrons/cm^2 [7]. Accumulation of a high density two-dimensional electron gas (2DEG) is due to the formation of a deep spike-shaped quantum well at the heterojunction, where there is a large conduction-band offset as well as a large discontinuity in the piezoelectric and spontaneous polarization [8]. For a successful design of advanced electronic devices based on AlGaN/GaN single heterojunctions, it is necessary to analyze the polarization effect and to characterize the dependence of subband structures using available material parameters. Many theoretical treatments of semiconductor heterostructures have been based on effective-mass Hamiltonians in the envelope-function approximation [9]-[15].

Previous studies [13]-[15] on subband calculations of AlGaN/GaN single heterojunctions have taken into account the piezoelectric and spontaneous polarization and the Hartree interaction of 2DEG. However, the exchange-correlation interaction, which represents the many-body effect, was not considered in earlier models for AlGaN/GaN single heterojunctions. Since the exchange-correlation interaction yields a considerable effect on the potential profile and subband energies of semiconductor heterostructure systems and leads to a large bandgap renormalization [11], it is necessary to take into account the many-body interaction for an accurate subband calculation of the AlGaN/GaN heterojunction with a high electron sheet concentration of about 1×10^{13} electrons/cm^2.

In the present paper, we report self-consistent numerical calculations for the subband structure of a Ga-face AlGaN/GaN single heterojunction. In the calculations we take into account the piezoelectric and spontaneous polarization and the many-body interaction including the Hartree and exchange-correlation potential energies. A basic formalism of the piezoelectric and spontaneous polarization in AlGaN/GaN heterojunctions is discussed in section II. A numerical method based on the effective mass approximation is described for subband calculations of AlGaN/GaN heterojunctions in section III. We discuss the influence of electron temperature and several structural parameters on the density and energies of 2DEG in the potential well at the heterojunction. Finally, a brief summary is given in section IV.

II. PIEZOELECTRIC AND SPONTANEOUS POLARIZATION

When a dielectric material is grown pseudomorphically on a substrate that has a different lattice constant, the grown layer will be strained and subjected to the piezoelectric polarization,

$$P_i^p = \sum_j e_{ij} \in_j , \tag{1}$$

where e_{ij} $(i=1,2,3; j=1,..,6)$ are the piezoelectric constants and $\in_j$ $(j=1,..,6)$ are the components of the strain field. For the case of AlGaN grown on a wurtzite GaN cladding layer, the AlGaN is under a biaxial tension, whose strain field is given as

$$\hat{\in} = (\in_1, \in_2, \in_3, 0, 0, 0), \tag{2}$$

where the strain-field components are given by

$$\in_1 = \in_2 = \frac{a_{strained} - a_{free}}{a_{free}}, \tag{3a}$$

$$\in_3 = \frac{c_{strained} - c_{free}}{c_{free}} = -\frac{2c_{11}}{c_{33}} \in_1 . \tag{3b}$$

Here, $(a_{strained}, c_{strained})$ and (a_{free}, c_{free}) are the lattice constants of the strained and the free-standing AlGaN crystals, respectively, and c_{ij} are the elastic stiffness constants. Since the piezoelectric tensor of wurtzite crystals has the following form [16]

$$\hat{e} = \begin{pmatrix} 0 & 0 & 0 & 0 & e_{15} & 0 \\ 0 & 0 & 0 & e_{14} & 0 & 0 \\ e_{31} & e_{31} & e_{33} & 0 & 0 & 0 \end{pmatrix}, \tag{4}$$

the piezoelectric polarization is given as

$$P^p = (0, 0, \; 2e_{31}\in_1 + e_{33}\in_3). \tag{5}$$

For an AlGaN layer grown on a Ga-face GaN cladding layer, the direction of the electric field in the AlGaN due to the piezoelectric polarization is towards the GaN layer along the (0001)-axis. For calculations of P_z^p in Al$_x$Ga$_{1-x}$N, we can use Vegard's rule for the elastic stiffness constants and the strain-field components in (5), e.g.,

$$\begin{aligned} P_z^{p,AlGaN} &= 2e_{31}^{AlGaN} \in_1^{AlGaN} + e_{33}^{AlGaN} \in_3^{AlGaN} \\ &= 2[xe_{31}^{AlN} + (1-x)e_{31}^{GaN}] \in_1^{AlGaN} \\ &\quad + [xe_{33}^{AlN} + (1-x)e_{33}^{GaN}] \in_3^{AlGaN}, \end{aligned} \tag{6}$$

where

$$\in_1^{AlGaN} = \frac{a^{GaN} - a^{AlGaN}}{a^{AlGaN}} \tag{7a}$$

and

$$\begin{aligned} \in_3^{AlGaN} &= -2 \frac{c_{11}^{AlGaN}}{c_{33}^{AlGaN}} \in_1^{AlGaN} \\ &= -2 \frac{xc_{11}^{AlN} + (1-x)c_{11}^{GaN}}{xc_{33}^{AlN} + (1-x)c_{33}^{GaN}} \in_1^{AlGaN} . \end{aligned} \tag{7b}$$

On the other hand, there is spontaneous polarization [8] in addition to piezoelectric polarization in wurtzite crystals. The spontaneous polarization in Al$_x$Ga$_{1-x}$N can also be estimated from Vegard's rule

$$P^{s,AlGaN} = xP^{s,AlN} + (1-x)P^{s,GaN} . \tag{8}$$

Therefore, for AlGaN/GaN single heterojunctions grown on a GaN buffer layer, the total polarization in the strained AlGaN is given by

$$P^{AlGaN} = P^{p,AlGaN} + P^{s,AlGaN}, \tag{9}$$

Table 1. Material parameters of $Al_xGa_{1-x}N$.

Parameters	Symbol	Unit	Value	References
Static Dielectric Constant	κ	ε_0	$8.5\,x + 10(1-x)$	[4]
Lattice Parameter	a	Å	$3.112\,x + 3.189(1-x)$	[17]
Lattice Parameter	c	Å	$4.982\,x + 5.185(1-x)$	[17]
Elastic Stiffness Constant	c_{11}	GPa	$435\,x + 377(1-x)$	[17][18]
Elastic Stiffness Constant	c_{12}	GPa	$125\,x + 160(1-x)$	[17][18]
Elastic Stiffness Constant	c_{13}	GPa	$120\,x + 114(1-x)$	[17][18]
Elastic Stiffness Constant	c_{33}	GPa	$395\,x + 209(1-x)$	[17][18]
Elastic Stiffness Constant	c_{44}	GPa	$118\,x + 8.14(1-x)$	[17][18]
Piezoelectric Constant	E_{31}	C/m^2	$-0.58\,x - 0.22(1-x)$	[19][20]
Piezoelectric Constant	E_{33}	C/m^2	$1.55\,x + 0.44(1-x)$	[19][20]
Spontaneous Polarization	P^s	C/m^2	$-0.081\,x - 0.029(1-x)$	[8]
Flat Conduction-Band Energy	V_c	EV	$0.7(2.12\,x + 0.6\,x^2)$	[1]
Electron Effective Mass	m*	m_e	$0.33\,x + 0.22(1-x)$	[21]
Donor-State Energy in AlGaN at the Flat Band Condition	E_D	eV	$V_c - 0.2$	
Acceptor-State Energy in GaN at the Flat Band Condition	E_A	eV	$V_c - 3.0$	

whereas the polarization of the unstrained GaN is

$$P^{GaN} = P^{s,GaN}. \qquad (10)$$

In a finite system, the existence of polarization implies the presence of an electric field. The electric field due to polarization is given as

$$F^{pol,A} = -\frac{P^A}{\kappa^A}, \qquad (11)$$

where A denotes AlGaN and GaN, and κ^A is the dielectric constant of material A.

Using the values of the material parameters of wurtzite AlGaN listed in Table 1, we calculate the piezoelectric and spontaneous polarization in the fully strained $Al_xGa_{1-x}N$ grown on the unstrained Ga-face GaN and the electric field strength that is due to the polarization as a function of the Al mole fraction. The calculated results in Fig. 1 show that both the piezoelectric polarization and the spontaneous polarization have negative values, indicating an accumulative effect in the total polarization. For the Ga-face AlGaN/GaN heterojunction, the electric field in AlGaN due to the polarization is directed along the (0001)-axis towards the GaN while the electric field
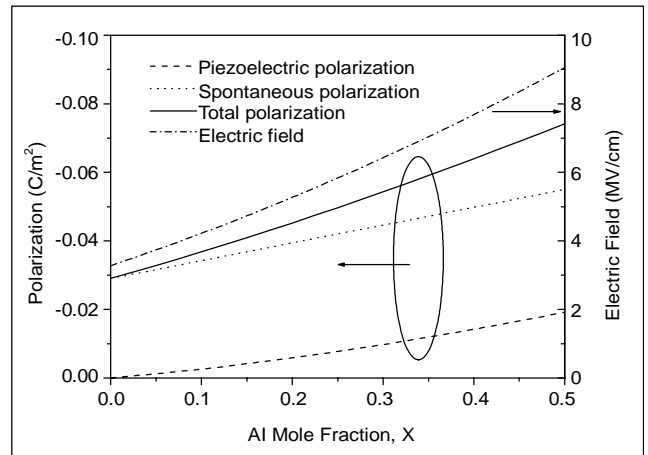

Fig. 1. The polarization in AlGaN grown on a Ga-face GaN cladding layer and the electric field strength due to polarization as a function of the Al mole fraction.

due to the spontaneous polarization in the GaN has the same direction as that in the AlGaN. The magnitude of the piezoelectric polarization shows a superlinear dependence on the Al mole fraction, whereas the spontaneous polarization reveals a linear behavior.

The accumulation of immobile polarization charges per unit area at the upper boundary of the AlGaN ($z = z_t$), at the AlGaN/

GaN heterojunction ($z=z_i$), and at the lower boundary of the GaN ($z=z_b$) are given by

$$\sigma(z_t) = P^{AlGaN}, \tag{12a}$$

$$\sigma(z_i) = P^{GaN} - P^{AlGaN}, \tag{12b}$$

and

$$\sigma(z_b) = -P^{GaN}, \tag{12c}$$

respectively. The calculated polarization charge density at the upper boundary of the AlGaN and at the AlGaN/GaN heterojunction are plotted as functions of the Al mole fraction in Fig. 2. If the electric field in AlGaN is completely cancelled either by a bias voltage of a Schottky contact on the AlGaN or by the electric field generated by ionized donor impurities, the charge density of positive polarization at the heterojunction can induce an equal negative charge density of electrons at the heterojunction region to form a 2DEG. For instance, the polarization charges at the $Al_{0.3}Ga_{0.7}N$/GaN heterojunction can induce the maximum electron sheet concentration of 1.58×10^{13} electrons/cm^2 at the heterojunction. Additional doping of donor impurities in AlGaN can raise the electron density while leaving ionized donors in the AlGaN, which will be discussed in detail in the next section.
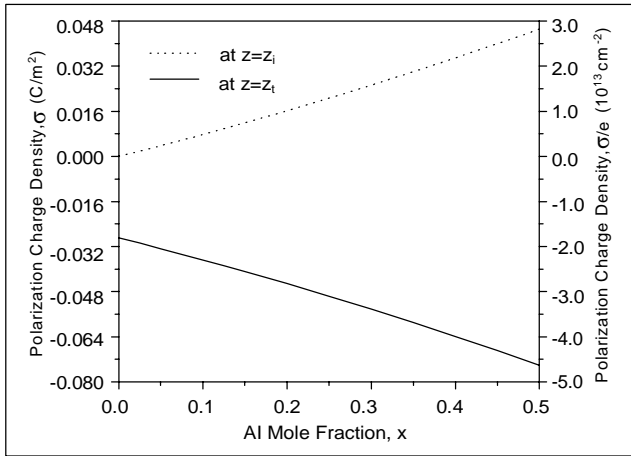

Fig. 2. Polarization charge density versus the Al mole fraction on the upper boundary of the AlGaN (the solid line) and at the AlGaN/GaN interface (the dotted line). Polarization charge density at the lower boundary of the GaN is 0.029 C/m^2 ($=1.81\times10^{13}$electrons/cm^2).

III. SUBBAND STRUCTURE

In the effective mass approximation, the electronic subband states in the growth direction of a single heterojunction are solutions to the Schrödinger equation,

$$-\frac{\hbar^2}{2}\frac{d}{dz}\left[\frac{1}{m^*}\frac{d\psi_i(z)}{dz}\right] + [V(z) - E_i]\psi_i(z) = 0, \tag{13}$$

where m^*, $V(z)$, and E_i are the electron effective mass at the conduction-band edge, the potential energy, and the energy of the i-th subband, respectively. Ignoring the conduction-band non-parabolicity, we assume that m^* is independent of electron energy and has an isotropic value changing abruptly at the interface between the AlGaN and GaN. The electron effective mass for the AlGaN is listed in Table 1. For instance, we use $m^* = 0.22m_0$ and $0.242m_0$ for the GaN and $Al_{0.2}Ga_{0.8}N$, respectively. $V(z)$ may be given as

$$V(z) = V_c(z) + V_H(z) + V_{xc}(z), \tag{14}$$

where $V_c(z)$ represents the conduction-band edge potential in a form of the step-function associated with the conduction-band offset at the AlGaN/GaN heterojunction, $V_H(z)$ is the Hartree potential of the electrostatic interaction due to mobile and immobile charges distributed in the system, and $V_{xc}(z)$ is the exchange-correlation potential representing the many-body interaction not included in the $V_H(z)$.

$V_H(z)$ is the solution to the Poisson equation,

$$\frac{d}{dz}\left[\kappa(z)\frac{d}{dz}V_H(z)\right] = e^2\rho(z), \tag{15}$$

where κ is the dielectric constant which is assumed to be changed abruptly at the AlGaN/GaN heterojunction. The density of total charges $\rho(z)$ is given as

$$\rho(z) = \sum_{j=t,i,b}\sigma(z)\delta(z - z_i) + p(z) + N_D^+(z) - n(z) - N_A^-(z), \tag{16}$$

where $\sigma(z)$, $p(z)$, N_D^+, $n(z)$, and N_A^- denote the density of immobile polarization charges, the density of free holes induced in the p-channels, the density of ionized donors, the density of free electrons in n-channels, and the density of ionized acceptors, respectively. For a system without a metal gate on the AlGaN barrier, a p-channel may be induced beneath the upper boundary of the AlGaN when the Fermi energy at the surface region lies in the valence band of the AlGaN, while for a system with a metal gate on the AlGaN, a p-channel may be induced in the metal when a bias voltage is applied between the gate and the electron channel. From the neutrality condition, the following conditions must be satisfied:

$$\int_{z_t}^{z_b}\rho(z)dz = 0 \tag{17}$$

for the sum of total charges and

$$\int_{z_t}^{z_b} [p(z) + N_D^+(z) - n(z) - N_A^-(z)]dz = 0 \qquad (18)$$

for the sum of mobile charges.

Considering AlGaN/GaN heterojunctions with one electron-gas channel formed at the heterojunction, $n(z)$ is given as

$$n(z) = \sum_i n_i |\psi_i(z)|^2, \qquad (19)$$

where n_i, the sheet density of electrons in the i-th subband, is given as

$$n_i = \frac{m^* k_B T}{\pi \hbar^2} \ln\left[1 + \exp\left(\frac{E_F - E_i}{k_B T}\right)\right]. \qquad (20)$$

Here, k_B and T are the Boltzmann constant and the electron temperature, respectively. The Fermi energy E_F is determined from the condition that the sum of subband electron densities is equal to the total electron density N_e:

$$N_e = \int_{z_t}^{z_b} n(z)dz = \sum_i n_i. \qquad (21)$$

N_e can be determined in a self-consistent manner using two boundary conditions for Fermi-level pinning at the upper and the lower boundaries of the system, as will be described below.

The density of positively ionized donors N_D^+ in (18) can be written as

$$N_D^+(z) = N_D(z) f_D^+(z), \qquad (22)$$

where $N_D(z)$ is the concentration of donor impurities distributed in the system, and $f_D^+(z)$ is the probability that a donor state with a degeneracy factor of 2 at energy $E_D(z)$ is ionized by losing an electron [22],

$$f_D^+(z) = 1 - \frac{1}{1 + \frac{1}{2}\exp\left[\dfrac{E_D(z) - E_F}{k_B T}\right]}. \qquad (23)$$

In AlGaN, it has been identified that N vacancy [23], Si, and O impurities [24] play the role of donors. In this report, however, we assume that $E_D(z)$ has a unique value of 0.2 eV below the conduction band of Al$_x$Ga$_{1-x}$N for all Al mole fractions. Since a 2DEG with a density of about 1×10^{13} electrons/cm^2 was achieved at a typical AlGaN/GaN single heterojunction without intentional doping in the AlGaN, it has been argued that most electrons are released from donor states formed at the top layer of the AlGaN [25].

N_A^- may also be given as

$$N_A^-(z) = N_A(z) f_A^-(z), \qquad (24)$$

where $N_A(z)$ is the concentration of acceptor impurities distributed in the system, and

$$f_A^-(z) = \frac{1}{1 + 4\exp\left[\dfrac{E_A(z) - E_F}{k_B T}\right]} \qquad (25)$$

is the probability that an acceptor state with a degeneracy factor of 4 at energy $E_A(z)$ is occupied by an electron [22]. In an AlGaN/GaN single heterojunction, the ionization or neutralization of acceptor states in the GaN buffer gives a significant effect on the potential profile in the buffer region, while acceptor states in the AlGaN layer cannat be easily neutralized at the thermodynamic equilibrium. There are several p-type dopants for GaN. For instance, Li, Be, Cd, Hg, Zn, and Mg are impurities playing the role of acceptor when they occupy Ga sites, whereas C and Si play the same role when they occupy N sites [1], [26]. In this report, however, we assume that acceptor impurities are distributed in the GaN and that $E_A(z)$ has a unique value of 3 eV below the conduction band of the material.

$V_{xc}(z)$ can be formulated using a density functional theory. In the simplest approximation, the so-called local density approximation (LDA) $V_{xc}(z)$ can be parameterized in an analytic form [27],

$$V_{xc}(z) = -\left[1 + \frac{0.7734 r_s}{21}\ln\left(1 + \frac{21}{r_s}\right)\right]\frac{2E_R}{\pi \alpha r_s}, \qquad (26)$$

where $\alpha = (4/9\pi)^{1/3}$, and r_s is the radius of a sphere containing one electron

$$r_s = \left[\frac{4}{3}\pi a^{*3} n(z)\right]^{-1/3} \qquad (27)$$

in the unit of the effective Bohr radius, and the effective Rydberg energy is given by

$$E_R = \frac{e^2}{8\pi \kappa a^*}. \qquad (28)$$

V_{xc} gives a significant effect on the electronic subband states and the bandgap with an increase of electron density [11].

The Schrödinger equation in (13) and the Poisson equation in (15) are calculated iteratively until a self-consistency is

achieved. For subband calculations, we consider a model AlGaN/GaN single heterojunction with the following boundary conditions:

i) If a metal Schottky gate is not on the AlGaN, the Fermi level is pinned at $e\varphi_t^0$ below the conduction band of the AlGaN in electrostatic equilibrium. On the other hand, with a metal gate on the AlGaN, the Fermi level is pinned at $e\varphi_t^1$ below the conduction band of the AlGaN at zero bias between the gate and the electron channel. However, in this report, we simply assume $e\varphi_t^0 = e\varphi_t^1 = 1.0$ eV.

ii) The AlGaN/GaN single heterojunction is grown on a GaN nucleation layer where the Fermi level is also assumed to be pinned at $e\varphi_b = 1$ eV below the conduction band of the GaN.

Figure 3 illustrates our model, depicting the calculated conduction-band profile, the amplitudes of wavefunctions of a few subbands at low energies, and the Fermi level in an Al$_{0.2}$Ga$_{0.8}$N/GaN single heterojunction for 35 nm thick AlGaN and 1.5 μm thick GaN layers. In the calculations, we assumed that $N_D(z) = N_A(z) = 0$ and T = 0 K. Taking into account the effect of the exchange-correlation interaction, we find that a thermodynamic equilibrium is achieved when 2DEGs with densities of 0.8364×10^{13} electrons/cm^2 and 0.0343×10^{13} electrons/cm^2 occupy the ground and second subbands, respectively, while the third subband is unoccupied. Since $N_D(z) = N_A(z) = 0$, all the electrons are released from the surface states where the Fermi level is pinned. The exchange-correlation potential in (26) has a spike-like shape, and its minimun value is calculated to be –49.6 meV at 1 nm from the junction in the GaN layer. The nonlinear potential profile of the AlGaN in the junction region as shown in Fig. 3 is in fact due to the exchange-correlation interaction. When the exchange-correlation interaction was not taken into account, the calculated electron sheet concentration was decreased by about 1 percent, while about 5 percent of the electrons in the ground subband were redistributed into the second subband, resulting in new electron densities of 0.8023×10^{13} electrons/cm^2 and 0.0621×10^{13} electrons/cm^2 in the ground and second subbands, respectively. These results reflect the significant influence of the exchange-correlation interaction of 2DEGs on the potential profile of the model AlGaN/GaN single heterojunction.

Figure 4 displays the dependence of electron sheet concentration on barrier width for two different Al mole fractions of 0.2 and 0.3, while other structural parameters are chosen to be the same as those of Fig. 3. As the barrier width is increased, the electron sheet concentration increases and

approaches the density of the polarization charges at the heterojunction, which is 1.0137×10^{13} electrons/cm^2 for $x = 0.2$ or 1.5805×10^{13} electrons/cm^2 for $x = 0.3$. On the other hand, as the barrier width is reduced, the electron sheet concentration decreases more rapidly, and eventually the density of the free electrons occupying the quasi two-dimensional (2D) channel at the AlGaN/GaN heterojunction becomes zero when the barrier width is less than a critical thickness which is determined by the Al mole fraction of the AlGaN. These results may be due to the fact that the energy of Fermi-level pinning at the top layer of the AlGaN should be independent of the width of the AlGaN. Consequently the
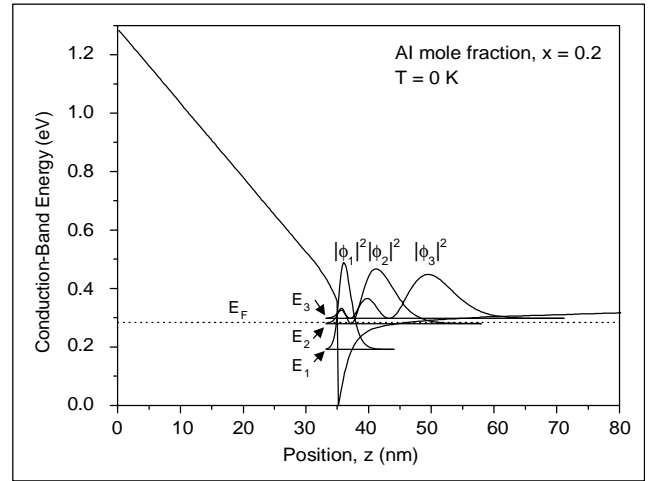

Fig. 3. Conduction-band profile of a model Al$_{0.2}$Ga$_{0.8}$N/GaN single heterojunction. We assumed that T = 0 K, the barrier width = 35 nm, the GaN width = 1.5 μm, and $N_D(z) = N_A(z)$=0. A thermodynamic equilibrium is achieved when 2DEGs with densities of 0.8364×10^{13} electrons/cm^2 and 0.0343×10^{13} electrons/cm^2 occupy the ground and second subbands, respectively.
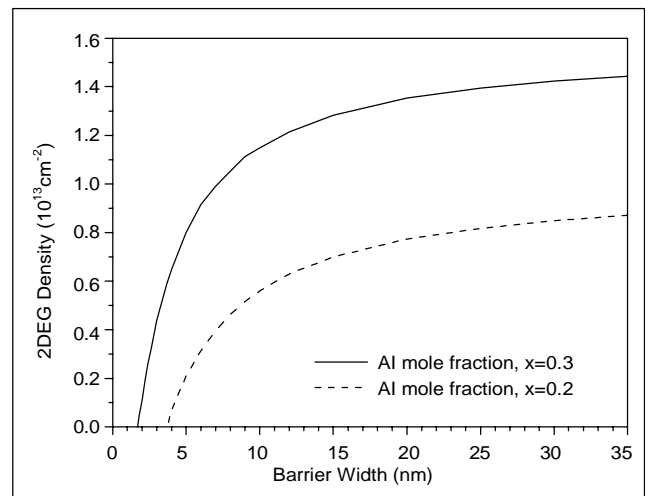

Fig. 4. Dependence of electron sheet concentration on Al$_x$Ga$_{1-x}$N width. It is assumed that the GaN width = 1.5 μm and $N_D(z) = N_A(z)$ =0.

potential energy difference due to the change of barrier width must be cancelled by a change of electron sheet concentration.

The dependence of electron sheet concentration on the width of GaN behaves in a way similar to the barrier-width dependence, i.e., it increases with the width of the GaN. The effect of the change of the GaN width on the electron sheet concentration is made by a change of the potential profile in the region of the electron channel. As the width of the GaN is increased, the electric field in the GaN decreases, resulting in decreases of both the subband energies and the Fermi energy. Therefore, in order to satisfy the boundary condition for Fermi-level pinning at the upper and lower boundary of the system, the electron density in the 2D channel needs to be increased as the width of the GaN is increased. However, for a typical $Al_{0.3}Ga_{0.7}N$/GaN single heterojunction with a 30 nm-wide AlGaN barrier, the electron sheet concentration is nearly saturated when the GaN is thicker than 100 nm.

A change in the Al mole fraction significantly influences the electron sheet concentration. Figure 5 depicts the dependence of electron sheet concentration on the Al mole fraction in the range of $x = 0$ to 0.4 for three different barrier thicknesses of 15, 30, and 50 nm. As the Al mole fraction is increased, electron density increases in nearly the same manner as the polarization charge density at the AlGaN/GaN heterojunctions does. The calculated results are in excellent agreement with some experimental data [28]-[31] measured on $Al_xGa_{1-x}N$/GaN single heterojunctions with a barrier width of 50 nm and

various Al mole fractions in the range of $x \leq 0.27$. However, it should be noted that those experimental data were obtained from unintentionally doped samples. On the other hand, the critical barrier width for maintaining the elastic strain in AlGaN grown on GaN decreases when the Al mole fraction is increased. Once the width of the AlGaN exceeds the critical thickness, the strain in the layer may be decreased. However, we assumed that AlGaN on a GaN buffer is elastically strained in the full range of our calculations; this may cause potential deviations of the calculated results from the experimental data for high Al mole fractions, $x > 0.3$.

In order to increase the electron sheet concentration in AlGaN/GaN single heterojunctions, the AlGaN can be doped intentionally with donor impurities. In Fig. 6, we plotted our calculated results for the dependence of the density of a 2DEG on doping density N_D in AlGaN for two different Al mole fractions of $x = 0.2$ and 0.3. We observe that electron sheet concentration increases when the doping density is increased. Our calculations also revealed that with an intentional doping with donor impurities in AlGaN, electron sheet concentration can be larger than the polarization charge density at the heterojunction. However, the contribution of additional donor impurities on the electron sheet concentration at the AlGaN/GaN heterojunction becomes less effective as the width of the AlGaN and the density of the donors in the AlGaN are increased. We also find that a heavy-doping of donor impurities in AlGaN reduces the effective width of the barrier and results in an increasing leakage current between the Schottky gate and the 2D channel of an electrical device.

On the other hand, the acceptor impurities in the GaN has a negligible effect on the density of 2DEG at the heterojunction.
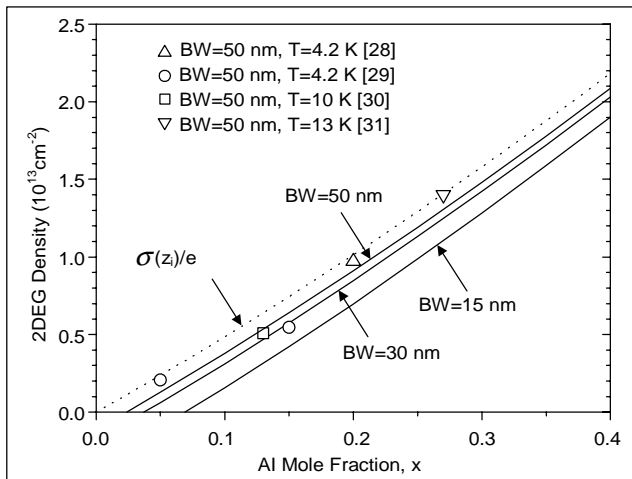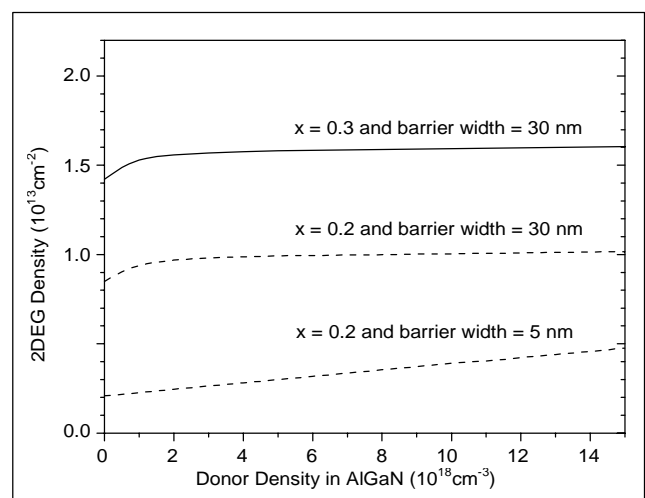

Fig. 5. Dependence of electron sheet concentration on the Al mole fraction of AlGaN for three different barrier widths (BW) of 15, 30 and 50 nm. The solid lines denote the calculated results, and the symbols represent the experimental results reported in [28]-[31], while the dotted line denotes the density of polarization charges at the AlGaN/GaN heterojunction. In the calculations, we assumed that the GaN width = 1.5 μm, $N_D(z) = N_A(z) = 0$, and T = 0 K.

Fig. 6. Dependence of electron sheet concentration on doping density N_D in $Al_xGa_{1-x}N$. We assumed the GaN width = 1.5 μm, $N_A(z) = 0$, and T = 0 K.

For instance, for a model structure with a GaN width of 1.5 μm, a barrier width of 30 nm, an Al mole fraction of 0.3, $N_D(z) = 0$, and T = 0 K, the calculated results plotted in Fig. 7 show that electron sheet concentration decreases by about 5 percent when the density of acceptors N_A in the GaN is increased from 0 to 10^6 cm^{-3}. However, the change of N_A in the GaN makes a significant effect on subband energies. As N_A is increased, the confinement effect of the spike-like potential well is enhanced especially for upper subbands other than the ground subband, resulting in a substantial increase in the energies of the upper subbands. In particular, with the present model system, we find that two subbands are occupied by 2DEGs when $N_A < 5 \times 10^{15}$ cm^{-3}, whereas only the ground subband is occupied when $N_A > 5 \times 10^{15}$ cm^{-3}. There are insignificant changes in subband energies and electron sheet concentration when the Fermi level is lower than the energy of the second subband.
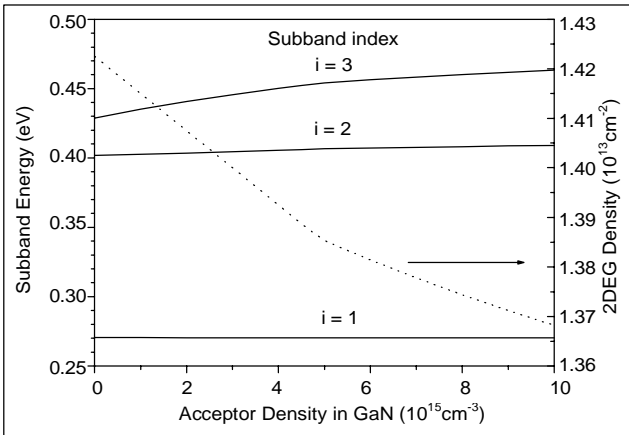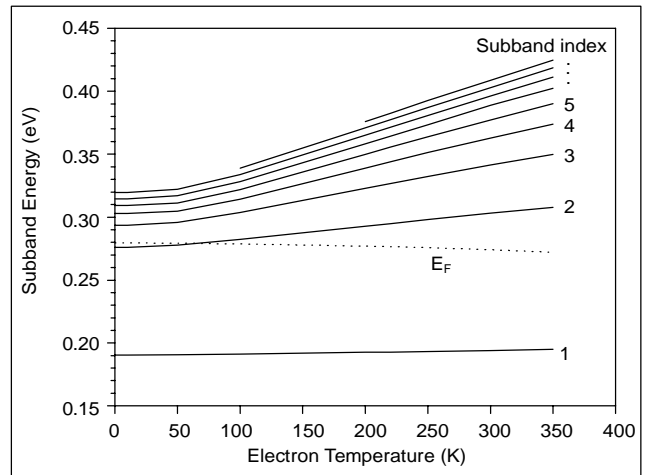

Fig. 8. The temperature dependence of subband energies and the Fermi energy. We assumed the GaN width = 1.5 μm, the barrier width = 30 nm, the Al mole fraction of AlGaN = 0.2, and $N_D(z) = N_A(z) = 0$.

Fig. 7. Dependence of subband energies and electron sheet concentration on acceptor density N_A in GaN. We assumed that the GaN width = 1.5 μm, the barrier width = 30 nm, the Al mole fraction = 0.3, $N_D(z) = 0$, and T = 0 K. For $N_A < 5 \times 10^{15}$ cm^{-3}, two subbands are occupied by 2DEGs, whereas for $N_A > 5 \times 10^{15}$ cm^{-3}, only the ground state is occupied.

As the electron temperature is increased, a number of subbands which are not occupied by a 2DEG at zero temperature can be occupied by free electrons because of the Fermi-Dirac statistics. This alters the potential well in such a way that the energies of the upper subbands increase while the Fermi level decreases (Fig. 8). In the calculations, we used a model AlGaN/GaN single heterojunction with a GaN width of 1.5 μm, a barrier width of 30 nm, an Al mole fraction of 0.2, and $N_D(z) = N_A(z) = 0$. The electron sheet concentration was rather insensitive to the change of the electron temperature. For instance, the electron sheet concentration in the system increases from 0.849×10^{13}

electrons/cm^2 to 0.850×10^{13} electrons/cm^2 as the electron temperature is increased from 0 K to 350 K. It should be noted that in a number of experiments a considerable increase of carrier densities has been observed from AlGaN/GaN single heterojunctions when the temperature was increased [29]. These experimental results are not consistent with our theoretical results. However, those experimental results could be due to the formation of bulk channels in addition to the 2DEG channel at elevated temperatures, which are not considered in our model.

IV. CONCLUSION

In summary, the conduction-band profile and subband structure of AlGaN/GaN single heterojunctions are calculated by a self-consistent numerical method. Piezoelectric and spontaneous polarization, as well as the many-body interaction, significantly affect the subband structure of AlGaN/GaN single heterojunctions. Electron sheet concentration at the AlGaN/GaN heterojunction is sensitively dependent on the Al mole fraction and the width of AlGaN and the doping density in the AlGaN barrier, while it is rather insensitive to the accepter concentration in the GaN layer and to the electron temperature. However, the acceptor concentration in the GaN and the electron temperature significantly affect the high energy subbands. The theoretical results of electron sheet concentration as a function of the Al mole fraction were in excellent agreement with some available experimental data available in the range of $x \leq 0.27$.

REFERENCES

[1] S. Strite and H. Morkoc, "GaN, AlN, and InN: a Review," *J. Vac. Sci. Technol. B*, vol. 10, no. 4, 1992, pp. 1237-1266.

[2] U.V. Bhapkar and M.S. Shur, "Monte Carlo Calculation of Velocity-Field Characteristics of Wurtizite GaN," *J. Appl. Phys.*, vol. 82, no. 4, 1997, pp. 1649-1655.

[3] S.M. Sze, *Physics of Semiconductor Devices*, John Wiley & Sons, New York, 1981, pp. 99-108.

[4] V.W.L. Chin, T.L. Tansley, and T. Osotchan, "Electron Mobilities in Gallium, Indium, and Aluminum Nitrides," *J. Appl. Phys.*, vol. 75, no. 11, 1994, pp. 7365-7372.

[5] Y.F. Wu, D. Kapolnek, J.P. Ibbetson, P. Parikh, B.P. Keller, and U.K. Mishra, "14-W GaN-Based Microwave Power Amplifiers," *2000 IEEE MTT-S Int'l Microwave Symp.*, Boston, MA, June, 2000, Piscataway, NJ [2000 IEEE MTT-S Int'l Microwave Symposium Digest, pp. 963-965].

[6] J.J. Xu, S. Keller, G. Parish, S. Heikman, U.K. Mishra, and R.A. York, "A 3-10-GHz GaN-Based Flip-Chip Integrated Broad-Band Power Amplifier," *IEEE Trans. Microwave Theory and Tech.*, vol. 48, no. 12, 2000, pp. 2573-2578.

[7] M. Asif Khan, A. Bhattarai, J.N. Kuznia, and D.T. Olson, "High Electron Mobility Transistor Based on a GaN-Al$_x$Ga$_{1-x}$N Heterojunction," *Appl. Phys. Lett.*, vol. 63, no. 9, 1993, pp. 1214-1215.

[8] F. Bernardini, V. Fiorentini, and D. Vanderbilt, "Spontaneous Polarization and Piezoelectric Constants of III-V Nitrides," *Phys. Rev. B*, vol. 56, no. 15, 1997, pp. R10024-R10027.

[9] G. Bastard, "Superlattice Band Structure in the Envelope-Function Approximation," *Phys. Rev B*, vol. 24, no. 10, 1981, pp. 5693-569.

[10] B.-W. Kim, Y.I. Jun, and H.B. Jung, "Envelope-Function Equation and Motion of Wave Packet in a Semiconductor Superlattice Structure, *ETRI J.*, vol. 21, no. 1, 1999, pp. 1-27; B.-W. Kim, J.-H. Yoo, and S.H. Kim, "An Improved Calculation Model for Analysis of [111] InGaAs/GaAs Strained Piezoelectric Superlattices," *ETRI J.*, vol. 21, no. 4, 1999, pp. 65-82.

[11] F. Stern and S.D. Sarma, "Electron Energy Levels in GaAs-Ga$_{1-x}$Al$_x$As Heterojunctions," *Phys. Rev. B*, vol. 30, no. 2, 1984, pp. 840-848.

[12] K.-S. Lee and E.-H. Lee, "Theoretical Investigations of the Effect of a Magnetic Field on the Landau-Level Structure of a Modulation-Doped Single Heterojunction Having Two Occupied Subbands," *Phys. Rev. B*, vol. 51, no. 19, 1995, pp. 13315-13319; K.-S. Lee and E.-H. Lee, "Optical Determination of the Heavy-Hole Effective Mass of (In,Ga)As/GaAs Quantum Wells," *ETRI J.*, vol. 17, no. 4, 1996, pp. 13-24.

[13] Y. Zhang and J. Singh, "Charge Control and Mobility Studies for an AlGaN/GaN High Electron Mobility Transistor," *J. Appl. Phys.*, vol. 85, no. 1, 1999, pp. 587-594.

[14] O. Ambacher, J. Smart, J.R. Shealy, N.G. Weimann, K. Chu, M. Murphy, R. Dimitrov, L. Wittmer, M. Stutzmann, W. Rieger, and J. Hilsenbeck, "Two-Dimensional Electron Gases Induced by Spontaneous and Piezoelectric Polarization Charges in N- and Ga-face AlGaN/GaN Heterostructures," *J. Appl. Phys.*, vol. 85, no. 6,

[15] F. Sacconi, A.D. Carlo, P. Lugli, and H. Morkoc, "Spontaneous and Piezoelectric Polarization Effects on the Output Characteristics of AlGaN/GaN Heterojunction Modulation Doped FETs," *IEEE Trans. Elec. Devices*, vol. 48, no. 3, 2000, pp. 450-457.

[16] W.G. Cady, *Piezoelectricity*, Dover, New York, 1964, Chap. VIII.; C. Shi, P.M. Asbeck, and E.T. Yu, "Piezoelectric Polarization Associated with Dislocations in Wurtzite GaN," *Appl. Phys. Lett.*, vol. 74, no. 4, 1999, pp. 573-575.

[17] J.H. Edgar, *Properties of Group III Nitrides*, INSPEC, London 1994, Chap. 1.

[18] R.B. Schwarz, K. Khachaturyan, and E.R. Weber, "Elastic Moduli of Gallium Nitride," *Appl. Phys. Lett.*, vol. 70, no. 9, 1997, pp. 1122-1124.

[19] J.G. Gualtieri, J.A. Kosinski, and A. Ballato, "Piezoelectric Materials for Acoustic Wave Applications," *IEEE Trans. Ultrasonics, Ferroelectrics, and Freq. Control*, vol. 41, no. 1, 1994, pp. 53-59.

[20] A.D. Bykhovsky, B.L. Gelmont, and M.S. Shur, "Elastic Strain Relaxation and Piezoeffect in GaN-AlN, GaN-AlGaN, and GaN-InGaN Superlattices," *J. Appl. Phys.*, vol. 81, no. 9, 1997, pp. 6332-6338.

[21] J.A. Majewski, M. Staedele, and P. Vogl, "Electronic Structure of Biaxially Strained Wurtzite Crystals GaN and AlN," *Mater. Res. Soc. Proc.*, vol. 449, Pittsburgh, PA, 1997, pp. 887-892.

[22] S.M. Sze, *Physics of Semiconductor Devices*, John Wiley & Sons, New York, 1981, pp. 22-27.

[23] J. Neugebauer and C. Van de Walle, "Atomic Geometry and Electronic Structure of Native Defects in GaN," *Phys. Rev. B*, vol. 50, no. 11, 1994, pp. 8067-8070.

[24] C.H. Park and D.J. Chadi, "Stability of Deep Donor and Acceptor Centers in GaN, AlN, and BN," *Phys. Rev. B*, vol. 55, no. 19, 1997, pp. 12995-13001.

[25] B.K. Ridley, "Polarization-Induced Electron Populations," *Appl. Phys. Lett.*, vol. 77, no. 7, 2000, pp. 990-992.

[26] S.N. Mohammad and H. Morkoc, "Progress and Prospects of Group-III Nitride Semiconductors," *Progress Quantum Electronics*, vol. 20, no. 5/6, 1996, pp. 361-525.

[27] L. Hedin and B.I. Lundqvist, "Explicit Local Exchange-Correlation Potentials," *J. Phys. C*, vol. 4, 1971, pp. 2064-2083.

[28] R. Gaska, J.W. Yang, A. Osinsky, Q. Chen, M. Asif Khan, A.O. Orlov, G.L. Snider, and M.S. Shur, "Electron Transport in AlGaN-GaN Heterostructures Grown on 6H-SiC Substrates," *Appl. Phys. Lett.*, vol. 72, no. 6, 1998, pp. 707-709.

[29] L.W. Wong, S.J. Cai, R. Li, K. Wang, H.W. Jiang, and M. Chen, "Magnetotransport Study on the Two-Dimensional Electron Gas in AlGaN/GaN Heterostructures," *Appl. Phys. Lett.*, vol. 73, no. 10, 1998, pp. 1391-1393.

[30] A. Saxler, P. Debray, R. Perrin, S. Elhamri, W.C. Mitchel, C.R. Elsass, I.P. Smorchkova, B. Heying, E. Haus, P. Fini, J.P. Ibbetson, S. Keller, P.M. Petroff, S.P. DenBaars, U.K. Mishra, and J.S. Speck, "Characterization of an AlGaN/GaN Two-Dimensional Electron Gas Structure," *J. Appl. Phys.*, vol. 87, no. 1, 2000, pp.

1999, pp. 3222-3233.

369-374.

[31] Y. Zhang, I.P. Smorchkova, C.R. Elsass, S. Keller, J.P. Ibbetson, S. Denbaars, U.K. Mishra, and J. Singh, "Charge Control and Mobility in AlGaN/GaN Transistors: Experimental and Theoretical Studies," *J. Appl. Phys.*, vol. 87, no. 11, 2000, pp. 7981-7987.

Kyu-Seok Lee received his BS and MS degrees from Yonsei University in 1979 and 1981, respectively, and PhD degree in physics from Northeastern University in 1990. He was a Research Associate at Northeastern University (1990) and spent a postdoctoral year (1991-92) at the Institute of Physical and Chemical Researches in Saitama, Japan. Since 1992, he has been with Electronics and Telecommunications Research Institute and is currently a Principal Member of Research Staff, in charge of a five-year research project for the development of GaN HFET devices for high-power and high-speed electronic applications. His main research interests have been on the optical and transport properties of semiconductors, physical phenomena in high magnetic fields, queueing problems in communications networks, InP-based opto-electronic devices and III-nitride electronic devices. He has authored and co-authored some 50 papers in scientific journals.

Doo-Hyeb Yoon received his BS and MS degrees in solid-state physics from Pusan National University, Busan, Korea in 1986 and 1988, respectively, and PhD degree in materials science from Tokushima National University, Tokushima, Japan in 1999. Before joining ETRI in 2001, he was with LG Central Research Institute for ten years (1988-1996 and 2000-2001) and with Optel Research Institute for one year (1999-2000). His research interests include fabrication of AlGaN/GaN HEMTs, fabrication of III-V nitrides laser diodes (LDs) and light-emitting diodes (LEDs), analysis of III-nitrides using atomic force microscopy, double crystal x-ray diffraction, transmission electron microscopy, and optical spectroscopy. He is a member of the Japan Society of Applied Physics.

Sung-Bum Bae received the BS and MS degrees in electronic engineering from Kyungpook National University (KNU), Daegu, in 1997 and 1999, respectively. He joined ETRI in 2001, while pursuing the PhD degree at KNU in the field of Metal Organic Chemical Vapor Deposition (MOCVD) of compound semiconductors. His research interests include growth of III-nitride semiconductors and design of field-effect transistors (FET) for high-power and high-frequency applications.

Mi-Ran Park received the PhD degree in electrical engineering from the University at Buffalo, in 2000. Her PhD thesis was entitled "Ohmic Contacts for Wide Bandgap Semiconductors: Processing, Properties and Mechanisms". While pursuing the PhD degree, her research interests focused on fabrication, characterization, and applications of ZnSe and GaN devices. She is currently a Senior Member of Research Staff at Electronics and Telecommunications Research Institute and involved in developing high frequency and high power AlGaN/GaN high electron mobility transistors.

Gil-Ho Kim Photograph and biography not available at the time of publication.